Methane Capture at Room Temperature: Adsorption on cubic δ-MoC and orthorhombic β-Mo_2C Molybdenum Carbides (001) Surfaces

Sergio Posada-Pérez,[a] José Roberto dos Santos Politi,[b] Francesc Viñes,[a,*] and Francesc Illas[a]

[a] *Departament de Química Física & Institut de Química Teòrica i Computacional (IQTCUB), Universitat de Barcelona, c/ Martí i Franquès 1, 08028 Barcelona, Spain.*

[b] *Universidade de Brasília, Instituto de Química, Laboratório de Química Computacional, CP 04478, Brasília, DF, 70904-970, Brazil.*

*Corresponding author: francesc.vines@ub.edu

Abstract

Based on periodic Density Functional Theory (DFT) calculations, carried out using a standard generalized gradient approximation type exchange-correlation functional including or not a van der Waals dispersive forces, the ability of the cubic δ-MoC(001) surface to capture methane at room temperature is suggested. Adsorption on the orthorhombic β-Mo_2C(001) surfaces, with two possible terminations, has been also considered and, in each case, several molecular orientations have been tested with one, two, or three hydrogen atoms pointing towards the surface on all high-symmetry adsorption sites. The DFT results indicate that the δ-MoC(001) surface shows a better affinity towards CH_4 than β-Mo_2C(001). The calculated adsorption energy values on δ-MoC(001) surface are larger, and hence better, than on other methane capturing materials such as metal organic frameworks. Besides, the theoretical desorption temperature values estimated from the Redhead equation indicate that methane would desorbs at 330 K when adsorbed on the δ-MoC(001) surface, whereas this temperature is lower than 150 K when the adsorption involves β-Mo_2C(001). Despite of this, adsorbed methane presents a very similar structure compared to the isolated molecule, due to a weak molecular interaction between the adsorbate and the surface. Therefore, the activation of methane molecule is not observed, so these surfaces are, in principle, not recommended as possible methane dry reforming catalysts.

Keywords: Density Functional Theory Calculations • Molybdenum Carbides • Methane Adsorption • Van der Waals Dispersion • Desorption • Methane Sequestration

Introduction

The rather stringent terms of the Kyoto protocol have triggered that the governments of many countries have committed to reduce the emission of greenhouse effect gases. In spite of this, the predictions indicate that these emissions will continue increasing up to 2040[1] with devastating consequences in the so-called global climate change. Since carbon dioxide (CO_2) is the most abundant gas in the Earth's atmosphere,[2] it is usually considered as the main causative of the greenhouse effect. However, methane (CH_4) can retain 23 times more heat than CO_2, consequently this fact must be taken into account, insomuch as methane emissions are five times lower.[2]

Due to its chemical properties and its danger to harm the environment, CH_4 has emerged as a molecule of interest, specially, in terms of gaining a material for its storage. In this ambit, porous materials, such as Metal Organic Frameworks (MOFs),[3,4] have achieved good results, and, thus they have been proposed as environmental capture and storage materials and for the posterior usage of CH_4 as fuel.[5-10] However, it is very important to develop better and cost-effective technologies for methane capture and utilization, not only to reduce greenhouse gas emissions, but also to capture methane and use it as a clean energy source. Moreover, in the field of industry and green chemistry, one of the most important research goals during the last years has been the study of a large-scale chemical conversion of CH_4 into environmentally friendly chemical compounds. However, methane is the most stable alkane molecule, and, thus its activation is very difficult. However, once CH_4 is activated, it can be used in a variety of reactions, such as methane partial oxidation ($CH_4 + {}^1/_2O_2 \rightarrow CO + 2H_2$),[11-13] steam reforming ($CH_4 + 3H_2O \rightarrow CO + 3H_2$),[14,15] or methane dry reforming ($CH_4 + CO_2 \rightarrow 2CO + 2H_2$).[16-19] Because of this, the activation of CH_4 has been extensively studied using catalysts based on transition metals,[20,21] nickel being the most common metal among them,[22,] despite the fact that it has been determined in theoretical[24] and experimental studies[14] on single crystal surfaces that platinum could reduce the energy barrier of the rate-limiting reaction step which corresponds to the first C-H bond scission.

During the last decades, researchers have tried to find economical new materials with a much better catalytic activity than typical transition metal catalysts. In the current search of new catalysts, Transition Metal Carbides (TMCs) have arisen as an appealing choice because they are disclosed to be a cheap and technically feasible alternative to noble metals in heterogeneous catalysis. The attention to this class of materials has been

growing since the landmark work of Levy and Boudart[25] highlighting the similar catalytic properties of tungsten carbide and platinum for a variety of reactions, which make them ideal replacements to Pt-group based catalysts. Not surprisingly, the number of articles on these compounds has greatly increased in the recent years due to their important physical, chemical, and catalytic properties.[26]

Many experimental and theoretical investigations have explored the catalytic capability of several TMCs for a broad range of reactions.[27-31] One of the TMCs that has generated more interest in the latest times is Titanium Carbide (TiC). Rodríguez *et al*. have shown that TiC(001) is an excellent catalyst to dissociate H_2 molecule[32,33] and to oxidize CO.[34] Also, it has been found that TiC can be an excellent support, since it is able to enhance the electronic structure of Au and Cu metal nanoparticles supported onto,[35] thus displaying a superior catalytic power with respect the isolated metal nanoparticles. Au/TiC(001) and Cu/TiC(001) are excellent catalysts for the hydrogenation of olefins, the hydrodesulfurization of thiophene, and the adsorption and decomposition of SO_2.[36-40] However, one must point out that TiC is a cumbersome support to be used in practical applications due to the difficulty of anchoring metallic nanoparticles on the TiC surface on working conditions. Alternative materials are δ-MoC and β-Mo_2C because they are much more active and do not require special conditions for their synthesis.

In the last years, MoC and Mo_2C have been used for studying synthetic and reactive aspects associated to environmental processes.[41-43] It is worth pointing out that here we follow the notation convention defined by the Joint Committee on Power Diffraction Standards (JCPDS) data files,[44] in which hexagonal and orthorhombic Mo_2C are denoted α-Mo_2C and β-Mo_2C, respectively. Note, however, that some authors in the literature refer to orthorhombic Mo_2C as α-Mo_2C,[45-47] following an early definition by Christensen.[48] Very recently, orthorhombic β-Mo_2C(001)-Mo terminated surface (bulk space group: *Pbcn*)[49] has been proposed for CO_2 dissociation and the subsequent conversion to methanol ($CO_2 + 3H_2 \rightarrow CH_3OH + H_2O$).[50,51] Furthermore, β-Mo_2C(001)-C terminated surface and cubic δ-MoC(001) can activate the C-O bonds. In the field of CH_4 adsorption, Tominaga *et al.* have theoretically predicted[52] that CH_4 is dissociated on hexagonal α-Mo_2C (bulk space group: *P3m1*),[49] although the authors missed in defining this surface as β and not α, as happened as well with the experimental studies carried out by Oshikawa *et al.*[53]

Thereby, taking into account these appealing results, the interaction between CH_4 and cubic and orthorhombic molybdenum carbides (001) surfaces is put under light, to see whether one could propose these materials as methane dry reforming catalysts. In different experimental thermodynamic studies it has been determined that, in order to attain high syngas yields, methane dry reforming requires reaction temperatures higher than 600 K, although carbon deposition is produced during the reaction.[18,54] Noble metals as Pt, Rh, and Ru are highly active towards dry reforming reaction and they are more resistant to carbon formation than other transition metal catalysts. However, they are seldom used due to their exceedingly high cost. Despite of these impairments, interesting results were published, in which Mo carbides are extremely active catalysts for the dry reforming, partial oxidation, and steam reforming of methane, with an activity comparable to noble metal catalysts.[55,56]

For all the above-mentioned reasons, and the excellent results obtained by Tominaga *et al.,*[52] a theoretical study about the adsorption of CH_4 on clean molybdenum carbides (001) surfaces seems necessary and has been undertaken. In this first study, we intend to analyse the methane capture on cubic and orthorhombic molybdenum carbide (001) pristine surfaces. Note that by so we disregard other possible effects, such as the the promotion by means of adsorbed metal alkalis,[57] or the effect of surface defects, as found to be matter of interest in the catalytic activity of a surface, as found, for example, in similar compounds such titanium nitride.[58,59] These aspects, which can come to be important, are however out of the scope of the present study, and matter of future work.

The structure of the adsorbed CH_4 is determined exploring whether catalysts based on $Mo_nC(001)$ surfaces are able to activate, and eventually break, the C-H bond. The calculations provide a well-detailed panel about the geometry and energy of methane adsorption on these surfaces. Besides, the Density of States (DOS), Electron Localization Function (ELF), and Charge Density Difference (CDD) plots were investigated in pertinent cases to complete the adsorption framework. This information allows determining the type of adsorption and predicting the role that these surfaces can play in methane reformation. Moreover desorption temperatures have been calculated in order to ascertain the material capability for capturing methane.

Computational details

Periodic Density Functional Theory (DFT) calculations were carried out using the Perdew-Burke-Ernzerhof (PBE) exchange-correlation functional[60] within the Generalized Gradient Approximation (GGA), as implemented in VASP 5.3.3 code.[61] In

the applied methodology, the electronic density of the valence electrons is expanded in a plane-wave basis set and the effect caused by the core electrons on those in the valence region is described by the Projected Augmented Wave (PAW) method of Blöch,[62] as implemented by Kresse and Joubert.[63] A cutoff kinetic energy of 415 eV was used together with a 5×5×1 mesh of **k**-points, selected by means of the Monkhorst-Pack scheme to carry out the numerical integrations in the Brillouin zone.[64] These values were optimized in a previous work on these surfaces and were found to provide highly-accurate results.[65]

Surface slab models with four layers have been constructed by repetition of four unit cells of the optimized bulk structures along the surface dimensions —(2×2) supercell— and by the addition of a vacuum region of 10 Å width in the normal-to-surface direction. The final structures of methane adsorbed on the surfaces were obtained after the simultaneous full optimization of CH_4 and of the two outmost layers of the studied surfaces, *i.e.* (2+2) approach. All supercells contain 32 Mo atoms; cubic δ-MoC(001) contains 32 C atoms whereas the orthorhombic β-Mo_2C contains 16 C atoms. The cell dimensions are 8.75×8.75×18.75 Å for δ-MoC(001) and 12.12×10.46×14.75 Å for β-Mo_2C.[65] The Newton-Raphson algorithm was employed for the atomic structure optimization together with a convergence criterion of 0.01 eV $Å^{-1}$ for the forces acting on relaxed atoms. The electronic relaxation convergence criterion was set to 10^{-5} eV.

Because of its predictable weak interaction, the study of methane adsorption requires a correct description of the van der Waals interactions that raise from the electron density dynamic fluctuation, and that can play a key role in such a process. In order to consider this type of interaction, the D2 correction of Grimme[66] was used, as implemented in VASP code.

The adsorption energy (E_{ads}) has been calculated as:

$$E_{ads} = E_{CH_4/MoC} - (E_{CH_4} - E_{MoC}) \qquad (1)$$

where $E_{CH_4/MoC}$ is the energy of the CH_4 adsorbed on the surface, E_{CH_4} is the energy of an isolated molecule, and E_{MoC} is the energy of the clean relaxed MoC or Mo_2C surface. Within this definition, the more negative the E_{ads} value, the stronger the adsorption. E_{CH_4} is obtained by placing the molecule in a broken symmetry unit cell of 9×10×11 Å dimensions and carrying out a $\mathbf{\Gamma}$-point optimization.

With the purpose of a detailed assessment of the adsorption capability of these surfaces, different surface sites for CH_4 adsorption have been explored, which are presented on Figure 1. Top sites involve the adsorbate on-top of a surface atom. This site is present in all the studied surfaces; for instance Top C is found on δ-MoC(001) and β-Mo_2C(001)-C surfaces and Top Mo in δ-MoC(001) and β-Mo_2C(001)-Mo surfaces. Bridge sites are considered when the contact is above the bond between two surface atoms, and can involve either Mo-C, C-C, or Mo-Mo bonds. Hollow sites involve the adsorbate binding simultaneously several surface atoms. Particularly, on β-Mo_2C(001), there are different hollow sites depending whether the molecule is interacting with C or Mo atoms of the inner layers. For each of the sites described above, three possible adsorption CH_4 orientations have been tested; with one, two, or three hydrogen atoms aiming to the surface as seen in Figure 2. Considering the tested surfaces sites and the molecular orientations, more than 80 different adsorption structures have been explored for methane adsorption. For the sake of simplicity, the adsorbed conformations shall be labelled hereafter only by the methane configuration (H_1, H_2, and H_3), the adsorption surface (δ for δ-MoC(001), β(C) and β(Mo) for β-Mo_2C (001) C-terminated and Mo-terminated surfaces, respectively) and the site of adsorption. The adsorption sites are labelled as follow: h for hollow, tC for Top C, tMo for Top Mo and b for Bridge. For β-Mo_2C(001) the labels of hC and hMo have been added to distinguish the different hollow sites. Moreover, in some cases, a superindex is added to differentiate among topologically distinct sites within the same cell. To clarify any doubt, consider the adsorption of methane with one hydrogen directed to δ-MoC(001) surface on top M site; its label would be δ-H_1).

Based on the E_{ads} values, most favourable adsorption systems for each encompassed surface have been further analysed by means of the DOS, a Bader charge analysis,[67] ELF function, and CDD. The CDD plots have been obtained as in Eq. (2),

$$\Delta\rho = \rho_{A-B} - \rho_A - \rho_B \qquad (2)$$

where $\Delta\rho$ is the CDD, ρ_{A-B} is the electron density of the CH_4 on the surface, ρ_A is that of the surface after the adsorption but without the adsorbate, and ρ_B is that of CH_4 in the adsorption geometry without the substrate. The values used to represent the isosurfaces vary between 0.01 and 0.001 a.u.

The CH_4 vibrational frequencies changes induced by adsorption have been also determined through the construction and diagonalization of the Hessian matrix,

constructed by independent displacements of atoms by 0.03 Å. Desorption temperatures have been calculated using the Redhead equation:[68]

$$\frac{E_b}{R \cdot T_d^2} = A \exp^{\frac{E_b}{R \cdot T_d}} \qquad (3)$$

where R is the ideal gases constant, T_d is the desorption temperature, A is the preexponential factor, and E_b is the desorption activation energy including Zero Point Energy (ZPE) correction which is calculated by Formula 4,

$$E_{ZPE} = E + \sum_i^{NMV} \frac{1}{2} h\nu_i \qquad (4)$$

where E_{ZPE} is the ZPE corrected total energy, E is the total energy, NMV is the number of normal modes of vibration, h is Planck constant, and ν_i is the i^{th} vibrational frequency. Note that for Formula 3, and a first order desorption kinetics, as applies here for methane adsorption on the studied carbide surfaces, A can have values in between 10^8 to 10^{13}. To make use of the Redhead equation, it has been decided to use the flashier heating conditions, and, consequently, the 10^{13} value, despite this fringe value provides the lowest desorption temperatures.

Results and discussion

Before discussing the results of CH_4 adsorption, let us briefly analyse the results for the isolated, gas phase, molecule. The calculated C-H bond distance is 1.095 Å, in excellent agreement with the experimental value of 1.086 Å.[69] Moreover, results in Table 1 evidence that the difference between present and previous[70] PBE calculated and experimental frequencies is very small, mostly owing to, on one hand, the neglect of the anharmonic component on the vibrations, and, on the other hand, to the intrinsic accuracy of the employed method. The asymmetric stretching mode ($2T_2$) has values above 3000 cm^{-1} and the umbrella mode ($1T_2$) around 1280 cm^{-1}. The symmetric stretching mode ($1A_1$) reaches values slightly lower than 3000 cm^{-1}, and, finally, the flexion vibration (E) values move around 1200-1550 cm^{-1}.

CH_4 adsorption on β-Mo_2C(001)

The results about the CH_4 adsorption on β-Mo_2C(001) are listed in Table 2. The table encompasses both the site preferences and the adsorption energy values including vdW or not. Furthermore, the percentage of van der Waals contribution (%vdW) to the adsorption energy, and the desorption temperature have been estimated and reported.

Note in passing by that E_{ads} is slightly higher on Mo-termination compared to C-termination. Both surfaces display slightly higher adsorption energies of CH_4 compared to various Ni surfaces. Results obtained including a vdW description are -0.19 eV for Ni(110) and Ni(100) surfaces, -0.24 eV for Ni(533), and -0.31 for Ni(577).[71] On β-Mo_2C(001) the adsorbed molecule structure is almost indistinguishable from the one in gas phase which is similar to results for CH_4 on Ni surfaces. Consistent with the rather low adsorption energy values, the estimated desorption temperatures are also low, much lower than room temperature. Thus, this surface cannot be used as potential CH_4 storage material.

At this surface, the increase of C-H bond distances with respect to the isolated methane molecule are negligible in all the tested cases (less than 0.02 Å, see Supporting Information). Notwithstanding, the C-H bond distances slightly increase when the hydrogen atoms are pointing towards the surface. Clearly, in all these cases CH_4 is physisorbed. Most favourable adsorption geometries are represented in Figure 3. In the case of C termination, there exist two geometries degenerated in energy, with two or three hydrogen atoms pointing to the surface (Figure 3a and 3b), respectively, whereas in the case of Mo termination (Figure 3c), a distinct situation appears; when vdW correction is not included in the calculations, only a quarter of the tested geometries reach the most stable physisorbed state. The rest tend to reach other minima with adsorption energies of -0.03 eV at best and likely to be artefacts rather than physically meaningful structures. Nevertheless, when vdW correction is included, the majority of the tested geometries reach the most favourable adsorption geometry. This issue was not featured on C termination, yet another effect was noticeable; once vdW dispersion is turned on, the CH_4-surface distance can be reduced by ~1 Å in selected cases. Despite of this proximity to the surface, the molecular structure is not varied, i.e. the approach is carried out in a rigid fashion. Because of all these reasons, a proper vdW correction is necessary so as to study the methane adsorption on these surfaces, both from the structural and the energetic aspects. This fact is justified by the vdW contribution to the adsorption energy (85% on average). Curiously these results do not keep the trend encountered for CO_2 adsorption on these molybdenum carbide surfaces.[50] This is because here the effect of Grimme correction on the calculations only affects the energy adsorption value, without modification of the adsorbate structure.

The vibrational frequencies of the different configurations were calculated and are shown in Table 3. Most of vibrational frequencies decrease, probably due to a slightly

weakening of C-H bonds. This is especially interesting in the case of β(Mo)-H_2(tMo) for the two highest energy vibration modes (T_2 and A_1), whose frequency values shift considerably, by more than 250 cm^{-1}. In general, when the H atoms are pointing to the surface, the C-H bond distance increases very slightly in comparison of the rest C-H bonds, but in the case of β(Mo)-H_2(tMo) these differences are one order of magnitude larger with respect the other studied systems (see Supporting Information). As a result, a clear decrease of vibrational frequency values is observed.

The Bader charges analysis (see Supporting Information and Figure 4) indicates that the charge transfer when the molecule is adsorbed is essentially negligible, with values below 0.1 e, thus, within the method accuracy limit. ELF images show only a slight polarization of the electron density within the methane molecule, and neither metallic nor covalent bonding with the surface is observed. Despite of this, a slight redistribution charge is highlighted by CDD calculations as one can see in Figure 4. In the cases of β(Mo)-H_2(tMo) and β(C)-H_3(hC) one can observe a charge transfer from dz^2 Mo orbitals plus *s* orbitals of H atoms to p_z of methane C atom. Contrary, this charge transfer is not observed on β(C)-H_2(hC). In this adsorption mode, the Mo carbide surface does not transfer charge to the CH_4, and only a charge redistribution is observed between p_z Carbon atom and *s* orbitals of Hydrogen atoms. The CDD results are confirmed by the analysis of electronic structure based on DOS (Figure 5). In these sketches, the projected DOS (PDOS) of CH_4 are enlarged to facilitate the visualization. One can see that the adsorption conformations where the charge transfer is observed, the triple-degenerated Highest Occupied Molecular Orbitals (HOMO) of methane are found in between values of -5 and -6 eV with respect Fermi level, whereas in the case of β(C)-H_2(hC), they are localized at ~-4.5 eV. Indeed, this fact also evidences the existence of charge transfer on β(Mo)-H_2(tMo) and β(C)-H_3(hC), since the transferred charge occupies previously unoccupied orbitals, thus shifting the occupied ones to lower energies.

Overall, as a first approximation, one would not advise the use of any termination of β-Mo_2C(001) surface as a catalyst for methane dry reforming, since these surfaces are not able to activate the C-H CH_4 bond when adsorbing it. Note that a more solid argument would require a methane dehydrogenation reaction profile, as previously carried out on Pt an Cu surfaces.[72,73] However, such study is out of the scope of the present research, and matter of future work, although, according to the desorption temperature estimates shown in Table 2, these surfaces would adsorb CH_4 but only at

cryogenic temperatures, and probably the first C-H bond scission would require to overcome a higher energy barrier, and so, methane would desorb rather than dissociating, and this latter process could only be forced, *e.g.* by applying molecular beams.[72]

CH_4 adsorption on δ–MoC(001)

Let us now examine the case of CH_4 adsorption on δ-MoC (001) surface for which the procedure and analysis have been carried out as for the β-Mo_2C(001) surfaces and the results are summarized in Table 4. The calculated energy values show that on the δ-MoC(001) surface the adsorption is significantly stronger than on β-Mo_2C(001), independently whether the latter is terminated by Mo or C atoms. In spite of this, the C-H bond distance increments are similar to the β-Mo_2C(001) surfaces. As in the case of the C-terminted β-Mo_2C(001) surface, there are two degenerated adsorption geometries with two (Figure 6a) or three (Figure 6b) H atoms pointing towards the surface. The distance between the C and Mo is around ~3 Å, while between one of the H atoms and surface C atoms is around ~2.5 Å.

The results in Table 4 imply that CH_4 becomes physisorbed on δ-MoC(001); the adsorption energy value is, without vdW and for all the tested geometries, ~-0.54 eV. Note that, despite the value is still small, the electronic bonding is significant, even larger than the bonding strength on β-Mo_2C(001) surfaces including the vdW correction. Still, even for the closest distance the Bader analysis reveals no clear charge transfer in between the molecule and the surface. Obviously, similar to the case of CH_4 adsorption on β-Mo_2C(001) surfaces, these results show that δ-MoC(001) surface is, in terms of CH_4 sequestration and its posterior treatment, a better catalyst than many Ni surfaces.[71] When vdW correction is included in the calculations, the E_{ads} value obviously increases in all the tested systems. However, for this surface, the E_{ads} is dominated by electrostatic contribution, contrary to what happens with the β-Mo_2C(001) surfaces . The vdW contribution to the adsorption energy is in average, of 41%, to final values of ~-0.95 eV. One could expect that these values imply a chemisorption process. Nevertheless, the CH_4 structure did not vary in comparison to the calculations without vdW dispersion. The increment in adsorption energy value is only due to the inclusion of vdW correction and no new interactions emerge.

The estimated desorption temperature values indicate that δ-MoC (001) is able to capture methane at room temperature, which would suggest that δ-MoC can be

considered as a CH_4 sequestration material. In order to corroborate these results, the adsorption energy values were compared with experimental and theoretical studies,[4,74] which used MOFs as a methane sequestration material. The adsorption energy value for these systems are -0.32 eV at best case. Therefore, δ-MoC(001) surface seems to be a much better material for methane sequestration. This necessary step is also vital for eventual CH_4 dissociation, although, as above commented, further studies on this matter are needed to propose this surface also for methane dry reforming.

To complete this study the vibrational frequencies and electronic structure analysis were performed using the same methodology as in β-Mo_2C(001) surfaces. One can expect that charge transfer results would vary with the support, since the adsorption energy differences and the capacity of capture CH_4 between δ-MoC(001) and β-Mo_2C(001) surfaces is notable. The vibrational frequencies are reported in Table 5. Almost all frequencies present a red shift when the molecule is adsorbed, i.e. the vibrational modes lower their frequency energy after the adsorption. Despite the adsorption energy values on δ-MoC(001) are higher than on β-Mo_2C(001) surfaces, the C-H bond distance increment is higher in the second case, and, as a result, the vibrational frequency values are lower when CH_4 is adsorbed on β-Mo_2C(001) surfaces. This is somewhat unpredictable, since in general one could think that C-H bonds should be weaker when the adsorption is stronger, as happens when is adsorbed on δ-MoC(001). The reason behind this behaviour is the subtle interplay between Pauli repulsion, generally increasing vibrational frequency, and charge transfer to the adsorbate which has the opposite effect.[75,76]

In spite of the fact that δ-MoC(001) is able to capture CH_4 and the adsorption energy values could be considered as chemisorption values, the Bader analysis present very similar results to β-Mo_2C(001) (see Supporting Information). Moreover, the ELF sketches (Figure 7) do not show any indication of bonding with the surface but still a slight electron density polarization. However, the CDD calculations show a charge redistribution as happened on β-Mo_2C(001) surface. The C atom of adsorbed CH_4 on δ-H_2(tMo) and δ-H_3(tMo) systems present a slight gain of electrons in their p_z orbitals, which receive this charge from a Mo atom on the surface. Nevertheless, except in the case of δ-H_3(h), charge transfer from surface to CH_4 is not observed. A more doubtful case is δ-H_3(tC), since a slight charge transfer exists, but this charge is reorganized on the substrate-molecule interface. Besides, the electronic structure (Figure 5) shows that in the cases of δ-H_3(h) and δ-H_3(tC), the PDOS of CH_4 is slightly closer to Fermi level

than δ-H_2(tMo) and δ-H_3(tMo). One could suggest that this result is again influenced by the charge transfer. In general terms though, the adsorption of methane does not perturb the electronic structure of δ-MoC.

Conclusions

An extensive theoretical study of the adsorption of CH_4 on cubic δ-MoC and orthorhombic β-Mo_2C (001) surfaces —the last one with C and Mo terminations— carried out at DFT level using the PBE functional has been presented. A van der Waals correction has been included to ascertain whether dispersive forces represent a key ingredient which has to be taken into account to properly describe these. Interestingly the most favoured methane adsorption conformation on δ-MoC(001) is not influenced by the van der Waals correction, but the opposite holds when considering CH_4 adsorption on the β-Mo_2C(001) surfaces. Regardless of the studied surface the interaction is always weak and can be safely classified as physisorption. Density of states and electron localization function plots show that this is the case independently of the methane adsorption conformation. A Bader analysis on the electron density confirms that there is essentially no charge transfer from the carbide surface to the CH_4, but CDD calculations suggest that a redistribution charge occurs on the majority of cases. Eventually, orthorhombic β-Mo_2C(001) surfaces do not present the same results that hexagonal α-Mo_2C(001) surface.

In spite of the lack of chemical interactions, on δ-MoC(001) reach values close to those corresponding to a chemisorption bond. However, none of the studied naked surfaces is able to activate the methane C-H bonds. Hence, even if recent work has shown that these surfaces efficiently activate CO_2, they do not constitute possible candidates for methane dry reforming catalysts.

The most striking prediction of the present work is that methane can remain adsorbed on δ-MoC(001) at room temperature. Besides, the predicted temperature desorption values are larger than those corresponding to other methane capture materials such as MOFs which makes δ-MoC(001) may be a potential candidate for methane capture.

Acknowledgements

The research carried out at the *Universitat de Barcelona* was supported by the Spanish MINECO grant CTQ2012-30751 grant and, in part, by *Generalitat de Catalunya* (grants 2014SGR97 and XRQTC). S. P. P. acknowledges financial support from Spanish MEC predoctoral grant associated to CTQ-2012-30751; F. V. thanks the MINECO for the postdoctoral *Juan de la Cierva* and *Ramón y Cajal* grants (JCI-2010-06372 and RYC-2012-10129); J.R.S.P. is thankful to CNPq for his postdoctoral fellowship; F. I. acknowledges additional support through the ICREA Academia award for excellence in research. Computational time at the *MARENOSTRUM* supercomputer has been provided by the Barcelona Supercomputing Centre through a grant from *Red Española de Supercomputación*.

Table 1: Experimental and calculated Vibrational frequencies for isolated methane molecule (ν) for all vibrational modes, in cm^{-1}.

ν	Calculated.		Experimental[70]
	Previous[70]	Present	
			3083
$2T_2$	3081	3158	3082
			3065
$1A_1$	2968	3037	2952
$1E$	1510	1567	1510
			1495
			1286
$1T_2$	1286	1357	1286
			1273

Table 2: Adsorption energy conformations, the corresponding adsorption energy values (including vdW correction or not), the percentage of vdW correction on the final adsorption energy value, and desorption temperature estimates for methane adsorbed on β-Mo_2C(001) surfaces. Energies are in eV and temperature in K.

Initial State	Final State	E_{ads}	E_{ads}+vdW	%vdW	T_d
β(C)-					
H_3(hC)	H_3(hC)	-0.05	-0.29	83	95
H_1(hC)	H_1(hC)	-0.04	-0.24	83	80
H_2(hC)	H_2(hC)	-0.05	-0.29	83	95
β(Mo)-					
H_2(hC^2)	H_2(tMo)	-0.11	-0.39	72	134
H_3(tMo)	H_2(tMo)[a]	-0.03	-0.39	92	134
H_1(hMo)	H_2(tMo)[a]	-0.03	-0.39	92	134

[a]These geometries are obtained only when vdW correction is included

Table 3: Vibrational frequencies (in cm^{-1}) for adsorbed methane molecule (ν) on β-Mo_2C(001) surfaces and shifts with respect CH_4 in vacuum (Δν).

Gas phase ν	ν[β(C)-H_3(hC)]	Δν	ν[β(C)-H_2(hC)]	Δν	ν[β(Mo)-H_2(tMo)]	Δν
3083	3061	-22	3095	12	3106	23
3082	3047	-35	3090	8	3033	-49
3065	3033	-33	3086	21	2778	-288
2952	2929	-23	2974	22	2700	-252
1510	1486	-24	1505	-5	1516	6
1495	1483	-12	1503	8	1423	-72
1286	1280	-6	1283	-3	1308	22
1286	1275	-11	1280	-6	1302	16
1273	1251	-22	1276	3	1145	-128

Table 4: Adsorption energy values and predicted desorption temperature for methane on the δ-MoC(001) surface. Energies are in eV and temperature in K

Initial State	Final State	E_{ads}	E_{ads}+vdW	%vdW	T_d
δ-H_3(h)	δ-H_3(h)	-0.54	-0.92	41	317
δ-H_3(tC)	δ-H_3(tC)	-0.54	-0.90	40	310
δ-H_2(tMo)	δ-H_2(tMo)	-0.54	-0.96	44	331
δ-H_3(tMo)	δ-H_3(tMo)	-0.55	-0.95	42	330

Table 5: Vibrational frequencies (ν) for adsorbed methane molecule on δ-MoC(001) surface, in cm^{-1}, and variation with respect CH_4 molecule in vacuum (Δν).

Gas phase ν	ν[δ-H_3(h)]	Δ ν	ν[δ-H_3(tC)]	Δ ν	ν[δ-H_2(tMo)]	Δ ν	ν[δ-H_3(tMo)]	Δ ν
3083	3085	2	3083	0	3084	1	3075	-8
3082	3081	-1	3073	-9	3067	-15	3073	-9
3065	3054	-11	3072	6	3044	-21	3070	5
2952	2953	1	2959	7	2943	-9	2955	3
1510	1507	-3	1502	-8	1509	0	1506	-4
1495	1497	2	1501	6	1505	11	1505	11
1286	1290	4	1285	-1	1293	7	1288	2
1286	1283	-3	1284	-2	1288	2	1285	-1
1273	1277	4	1281	7	1267	-7	1280	6

Figure 1: Sketches of the different methane adsorption sites tested for the three studied surfaces. Images show top views of a) δ-MoC, b) β-Mo_2C-C, and c) β-Mo_2C-Mo (001) surfaces. Violet and green balls denote Mo and C atoms, respectively. Red, orange, and blue marks denote Top, Hollow, and Bridge adsorption sites, respectively.

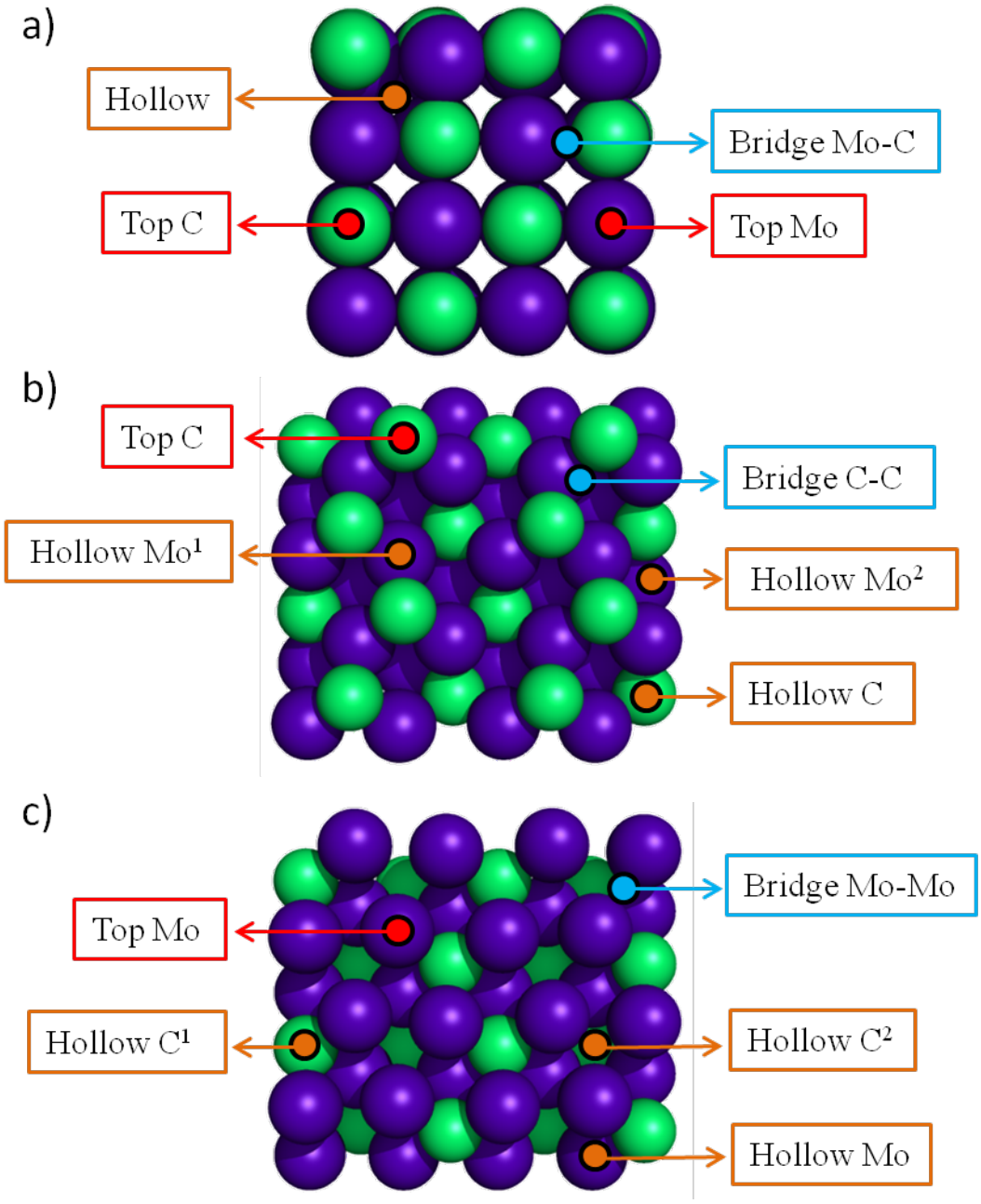

Figure 2: Sketches of the three different tested methane orientations. The images show methane molecules with 1 Hydrogen (left), 2 Hydrogen (middle), or 3 Hydrogen (right) atoms, pointing to the surface. Sphere colouring as in Figure 1.

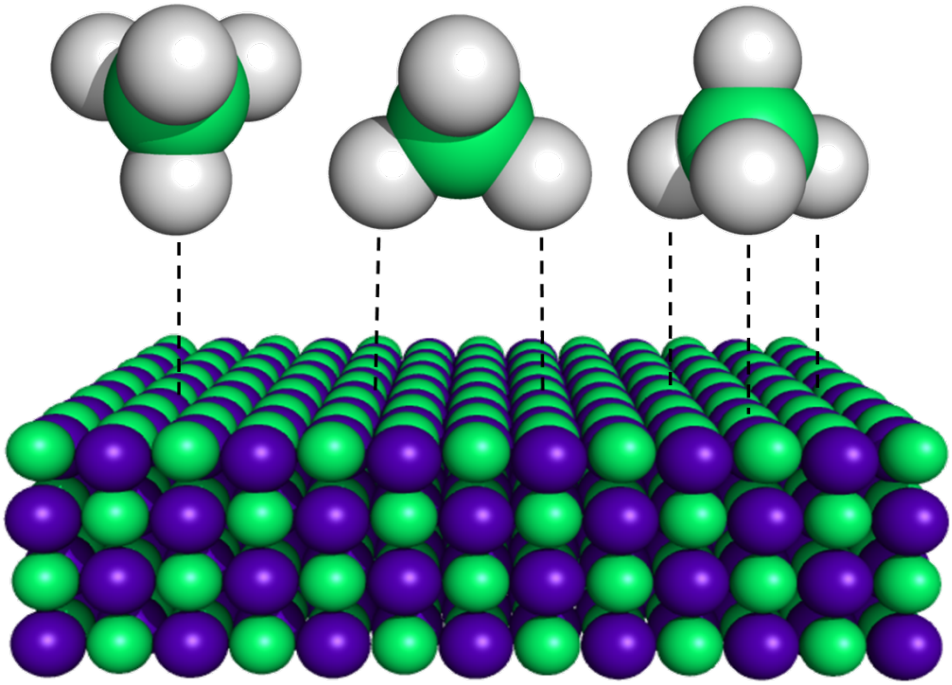

Figure 3: Most stable CH_4 adsorption geometries on β-Mo_2C(001)-C surface with a) two or b) three Hydrogen atoms aiming to the surface, and c) most stable structure on β-Mo_2C(001)-Mo. Side (top) and top views (bottom) are displayed. Sphere colouring is as in Figure 1.

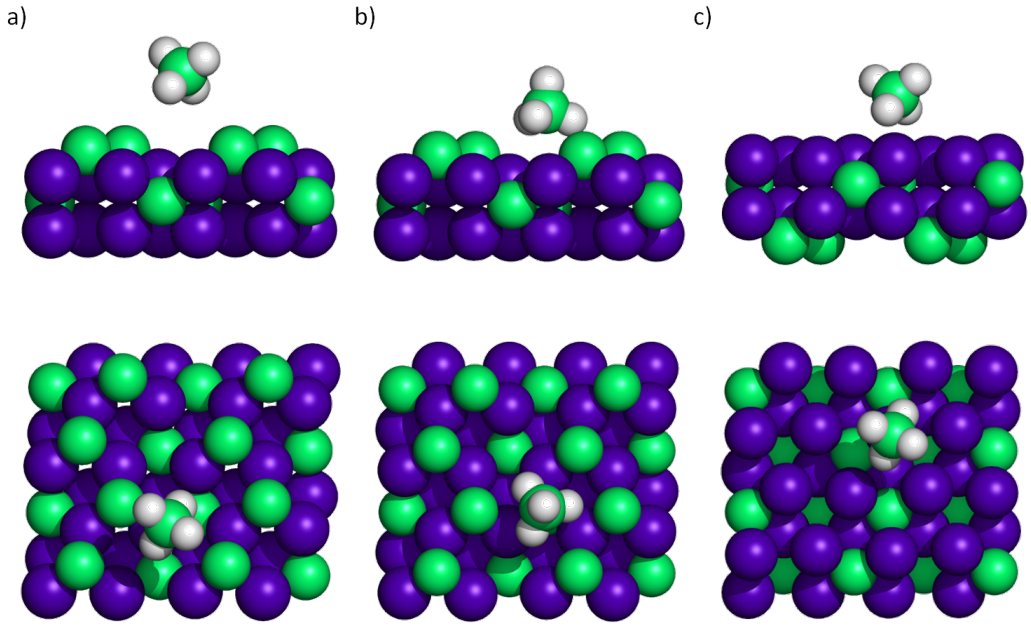

Figure 4: (a) ELF and (b) CDD images of most stable configurations of methane adsorbed on β-Mo_2C(001) surfaces. ELF planes have been turned from orthogonality for a better visualization of methane-surface interaction. Blue and green balls denote Mo and C atoms, respectively in (a). Yellow and black denote positive and negative density charge respectively in (b). Sphere colouring in (b) as in Figure 1.

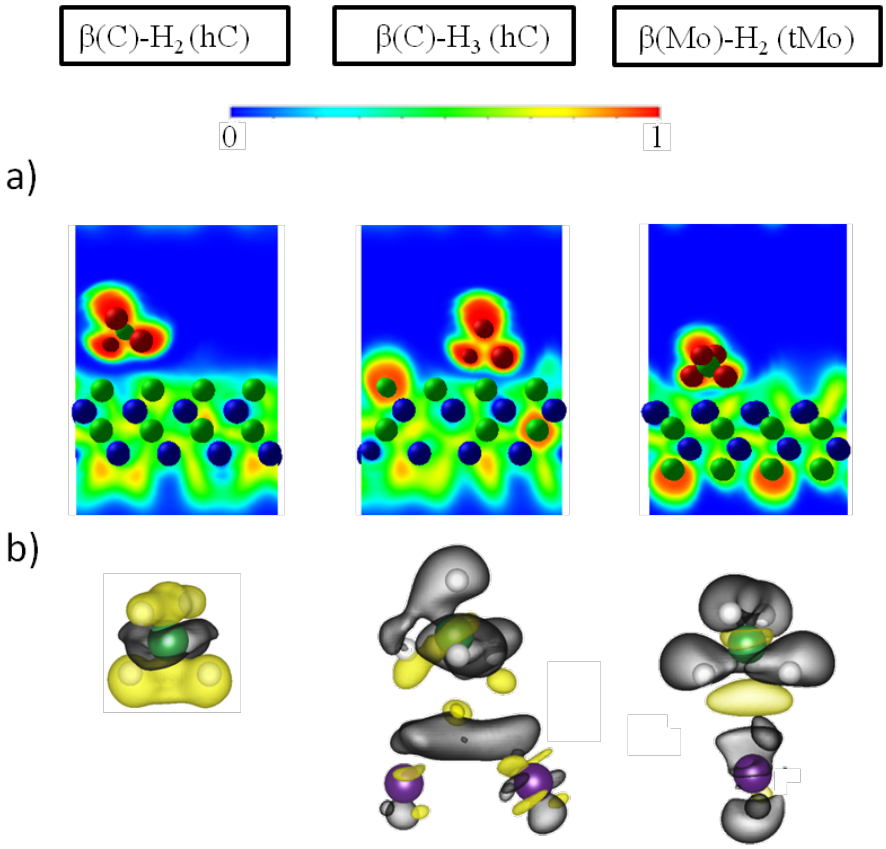

Figure 5: Projected DOS of methane adsorbed on β-Mo_2C and δ-MoC (001) surfaces. Methane PDOS has been amplified (left multipliers) in order to facilitate the visualization.

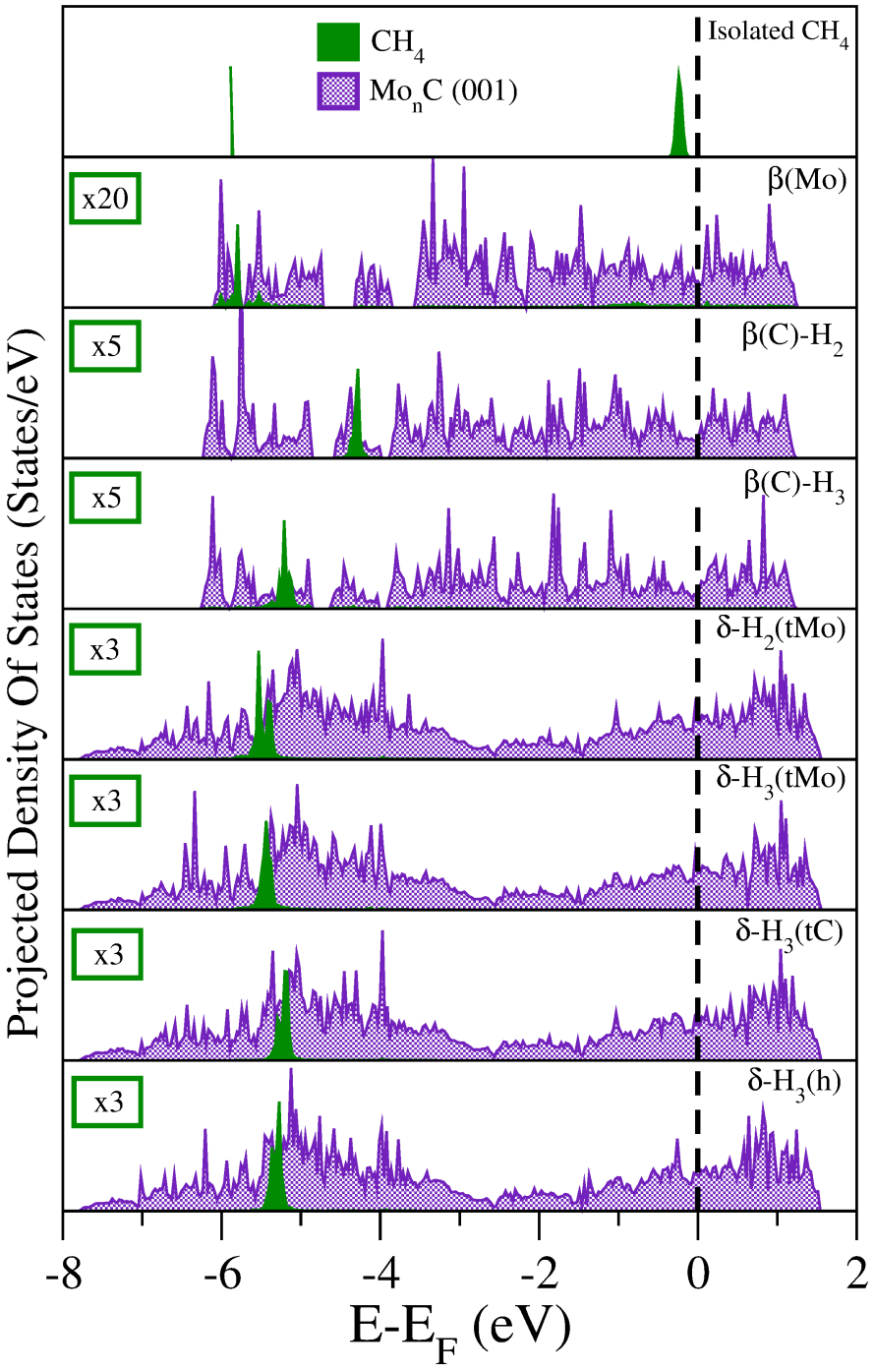

Figure 6: Views of the two most stable adsorption geometry of methane on δ-MoC(001) surface. The δ-H_2(tMo) (a) and δ-H_3(tMo) (b) adsorption conformations are shown. Side (top) and top views (bottom) are displayed. Sphere colouring as in Figure 1.

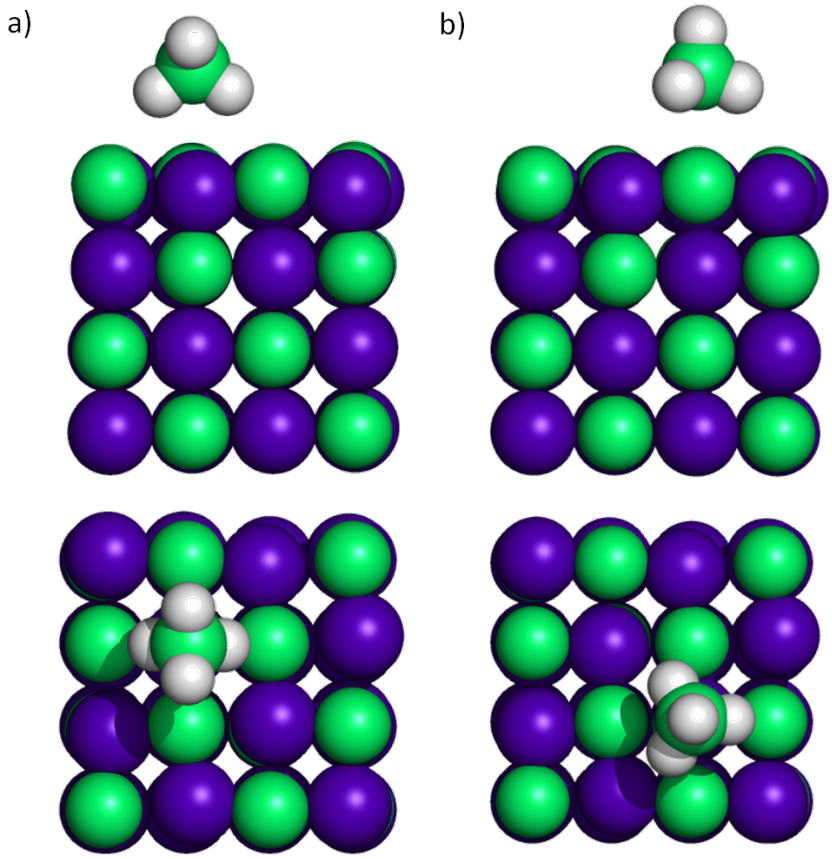

Figure 7: (a) ELF and (b) CDD images of most stable configurations of methane adsorbed on δ-MoC(001) surface. ELF and CDD colouring as in Figure 4.

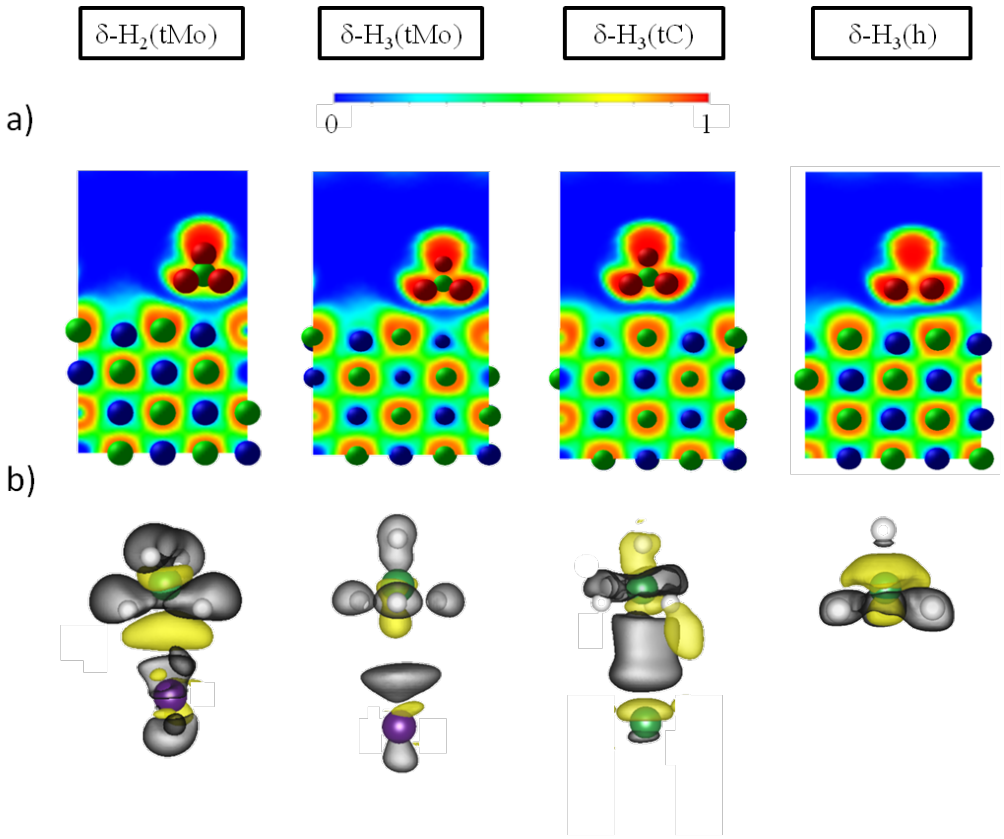

References

[1] U.E.I. Administration, International Energy Outlook 2013, Washington DC, 2013; http://www.eia.gov/forecasts/ieo/pdf/0484%282013%29.pdf.

[2] J. Feichter, U. Schurath, R. Zellner, *Chem. Unserer Zeit*, 2007, **41**, 138.

[3] M. Eddaoudi, J. Kim, N. Rosi, D. Vodak, J. Wachter, M. O'Keeffe, O. M. Yaghi, *Science*, 2002, **295**, 469.

[4] H. Wu, J. M. Simmons, Y. Liu, C. M. Brown, X. S. Wang, S. Ma, V. K. Peterson, P. D. Southon, C. J. Kepert, H. C. Zhou, T. Yildrim, W. Zhou, *Chem Eur. J.* 2010, **16**, 5205.

[5] M. H. Zhang, Y. Z. Yu, Y. B. Zhang, *App. Surf. Sci.*, 2013, **280**, 15.

[6] M. Nao, X. J. Fu, Y. Q. Lei, H.Q. Su, *Chin. J. Cat.*, 2013, **34**, 379.

[7] O. A. Berekentidou, M. A. Goula, *Catal. Today*, 2012, **195**, 93.

[8] T. A. Makal, J. R. Li, W. Lu, H. C. Zhou, *Chem. Soc. Rev.*, 2012, **41**, 7761.

[9] B. C. Wood, S. Y. Bhide, D. Dutta, V. S. Kandagal, A. D. Pathak, S. N. Punnathanam, K. G. Ayappa, S. Narasimhan, *J. Chem. Phys.*, 2012, **137**, 054702.

[10] S. J. Mahdizadeb, E. K. Goharshadi, *J. Nanopart. Res.*, 2013, **15**, 1393.

[11] M. Pettre, C. Eichner, M. Perrin, *J. Chem. Soc. Faraday Trans*,.1946, **43**, 335.

[12] D. A. Hickman, L. D. Schmidt, *Science*, 1993, **259**, 343.

[13] V. R. Choudhary, A. M. Rajput, B. Prabhakar, *J. Catal.* 1993, **139**, 326.

[14] F. Besenbacher, I. Chorkendoff, B. S. Clausen, B. Hammer, A. M.Molenbroek, J. K. Nørskov, I. Stensgaard, *Science*, 1998, **279**, 1913.

[15] J. P. Van Hook, *Catal. Rev. Sci. Eng.*, 1980, **21** ,1.

[16] A. T. Ashcroft, A. K. Cheetham, M. L. H. Green, P. D. F. Vernon, *Nature*, 1991, **352** , 225.

[17] M. C. Bradford, M. A. Vannice, *Catal. Rev. Sci. Eng.* 1999, **41**, 1.

[18] M. C. J. Bradford, M. A. Vannice, *Appl. Catal. A* 1996, **142**, 97.

[19] K. Tomishige, Y.-G. Chen, K. Fujimoto, *J. Catal.* 1999, **181**, 91.

[20] R. D. Beck, P. Maroni, D. C. Papageorgopoulos, T. T. Dang, M. P.Schmid, T. R. Rizzo, *Science* 2003, **302**, 98.

[21] A. C. Luntz, *Science*, 2003, **302**, 70.

[22] P. D. F. Vernon, M. L. H. Green, A. K. Cheetham, A. T. Ashcroft, *Catal. Today*, 1992, **13**, 417.

[23] R. Bisson, M. Sacchi, T. T. Dang, B. Yoder, P. Maroni, R. D. Beck, *J.Phys. Chem. A,* 2007, **111**, 12679.

[24] S. Nave, B. Jackson, *J. Chem. Phys.* 2009, **130**, 054701.

[25] R. B. Levy, M. Boudart, *Science*, 1973, **181**, 547.

[26] F. Viñes, C. Sousa, P. Liu, J. A. Rodriguez, F. Illas, *J. Chem. Phys.,* 2005, **122**, 174709.

[27] S. T. Oyama, *Catal. Today*, 1992, **15**, 179.

[28] H. Hwu, J. G. Chen, *Chem. Rev.*, 2005, **105**, 185.

[29] F. Viñes, J. A. Rodriguez, P. Liu, F. Illas, *J. Phys. Chem. C*, 2007, **111**, 1307.

[30] F. Viñes, C. Sousa, F. Illas, P. Liu, J. A. Rodriguez, *J. Phys. Chem. C*, 2007, **111**, 16982.

[31] A. Vojvodic, A. Hellman, C. Ruberto, B. I. Lundqvist, *Phys. Rev. Lett.*, 2009, **103**, 146103.

[32] J. A. Rodriguez, P. Liu, F. Viñes, F. Illas, Y. Takahashi, K. Nakamura, *Angew. Chem., Int. Ed*., 2008, **47**, 6685.

[33] J. A. Rodriguez, P. Liu, Y. Takahashi, K. Nakamura, F. Viñes, F. Illas, *J. Am. Chem. Soc*., 2009, **131**, 8595.

[34] J. A. Rodriguez, P. Liu, Y. Takahashi, K. Nakamura, F. Viñes, F. Illas, *Top. Catal.*, 2010, **53**, 393.

[35] J. A. Rodriguez, F. Viñes, F. Illas, P. Liu, Y. Takahashi, K. Nakamura, *J. Chem. Phys.*, 2007, 127, 211102.

[36] J. A. Rodriguez, P. Liu, F. Viñes, F. Illas, Y. Takahashi and K. Nakamura, *Angew. Chem. Int. Ed*., 2008, **47**, 6685.

[37] J. A. Rodriguez, P. Liu, Y. Takahashi, K. Nakamura, F. Viñes and F. Illas, *J. Am. Chem. Soc*., 2009, **131**, 8595.

[38] L. Feria, J. A. Rodriguez, T. Jirsak and F. Illas, *J. Catal.*, 2011, **279**, 352.

[39] J. A. Rodriguez, P. Liu, Y. Takahashi, K. Nakamura, F. Viñes and F. Illas, *Top. Catal.*, 2010, **53**, 393.

[40] J. A. Rodriguez, P. Liu, Y. Takahashi, F. Viñes, L. Feria, E. Florez, K. Nakamura, F. Illas, *Catal. Today*, 2011, **166**, 2.

[41] W. Zheng, T. P. Cotter, P. Kaghazchi, T. Jacob, B. Frank, K. Schlichte, W. Zhang, D. S. Su, F. Schüth, R. Schlögl, *J. Am. Chem. Soc.*, 2013, **135**, 3458.

[42] P. Liu, J. A. Rodriguez, *J. Phys. Chem. B*, 2006, **110**, 19418.

[43] M. Patel, M. A. S. Baldanza, V. Teixeira da Silva, A. V. Bridgwater, *App. Catal. A: General*, 2013, **458**, 48.

[44] *Powder Diffraction File*; JCPDS International Center for Diffraction Data: Pennsylvania, 2004.

[45] Ren, C.-F. Huo, J. Wang, Z. Cao, Y.-W. Li, H. Jiao, *Surf.Sci.*, 2006, **600**, 2329.

[46] H. Tominaga, Y. Aoki, M. Nagai, *Appl. Catal., A*, 2012, **423–424**, 192.

[47] H. Tominaga, M. Nagai, *J. Phys. Chem. B*, 2005, **109**, 20415.

[48] A. N. Christensen, *Acta Chem. Scand., Ser. A*, 1977, **31**, 509.

[49] E. Parthé, V. Sadagopan, *Acta Crystallogr.*, 1963, **16**, 202.

[50] S. Posada-Pérez, F. Viñes, P. J. Ramirez, A. B. Vidal, J. A. Rodriguez, F. Illas, *Phys. Chem. Chem. Phys.*, 2014, **16**, 14912.

[51] M. D. Porosoff, X. Yang, J. A. Boscoboinik, J. G. Chen, *Angew. Chem., Int. Ed*. 2014, **53**, 6705.

[52] H. Tominaga, M. Nagai, *Appl. Catal.*, A, 2007, **328**, 35.

[53] K. Oshikawa, M. Nagai, S. Omi, *J. Phys. Chem. B* 2001, **105**, 9124.

[54] G. S. Gallego, C. Batiot-Dupeyrat, J. Barrault, E. Florez, F. Mondragon, *Appl. Catal.*, A, 2008, **334**, 251.

[55] A. P. E. York, J. B. Claridge, A. J. Brungs, S. C. Tsang, M. L. H. Green, *Chem. Commun.*, 1997, **1**, 39.

[56] J. B. Claridge, A. P. E. York, A. J. Brungs, S. C. Tsang, M. L. H. Green, *J. Catal.*, 1998, **180**, 85.

[57] C. Pistonesi, M. E. Pronsato, L. Bugyi, A. Juan, *J. Phys. Chem. C*, 2012, **116**, 24573.

[58] R. Q. Zhang, C.-E. Kim, B. -D. Yu, C. Stampfl, A. Soon, *Phys. Chem. Chem. Phys.* 2013, **15**, 19450.

[59] T. Lee, B. Delley, C. Stampfl, A. Soon, *Nanoscale*, 2012, **4**, 5183.

[60] J. P. Perdew, K. Burke, M. Ernzerhof, *Phys. Rev. Lett.*, 1996, **77**, 3865.

[61] G. Kresse, J. Hafner, *Phys. Rev. B*, 1993, **47**, 558.

[62] P.E. Blöch, *Phys. Rev. B*, 1994, **50**, 17953.

[63] G. Kresse, D. Joubert, *Phys. Rev. B*, 1999, **59**, 1758.

[64] H. J. Monkhorst, J. D. Pack, Phys. Rev. B 1976, **13**, 5188.

[65] J. R. S. Politi, F. Viñes, J. A. Rodriguez, F. Illas, *Phys. Chem. Chem. Phys.*, 2013, **15**, 12617.

[66] S. Grimme, *J. Comput. Chem.*, 2006, **27**, 1787.

[67] R. F. Bader, *Atoms in Molecules: A Quantum Theory;* Oxford Science: Oxford, U.K., 1990.

[68] P. A. Redhead, *Vacuum* 1962, **12**, 203.

[69] D. L. Gray, A. G. Robiette, *Mol. Phys.*, 1979, **37**, 1901.

[70] D.C. Patton, D.V. Porezag, M.R. Pederson, *Phys. Rev. B*, 1997, **55**, 7454.

[71] S. González, F. Viñes, J. F. García, Y. Erazo, F. Illas, *Surf. Sci.*, 2014, **625**, 64.

[72] F. Viñes, Y. Lykhach, T. Staudt, M. P. A. Lorenz, C. Papp, H. P. Steinrück, J. Libuda, K. M. Neyman, A. Görling, *Chem. Eur. J.* 2010, **16**, 6530.

[73] W. Zhang, P. Wu, Z. Li, J. Yang, *J. Phys. Chem. C* 2011, **115**, 17782.

[74] Y. He, W. Zhou, G. Qian, B. Chen, *Chem. Soc. Rev.*, 2014, **43**, 5657.

[75] F.Illas, S.Zurita, J.Rubio and A.M. Marquez, *Phys. Rev. B*, 1995, **52**, 12372.

[76] F. Illas, S.Zurita, A.M. Marquez and J.Rubio, *Surf. Sci.*, 1997, **376**, 279.